Impact of substrates on heat capacity of lyophilised biomass of Fusarium oxysporum associated with cyanidation wastewater

Enoch Akinpelu[1], Seteno Ntwampe[2], Lukhanyo Mekuto[3], and Tunde Ojumu[3]

[1]North-West University
[2]North-West University - Potchefstroom Campus
[3]Cape Peninsula University of Technology

May 5, 2020

Abstract

Cyanide is a well-known constituent of mine wastewater which can be degraded by various process. However, due to cost and environmental challenges, microbial degradation seems to be the most effective process. When wastewater is treated with microorganisms, process performance should not only be based on toxicant degraded but also on the impact of the toxicant on the physical properties of the microorganisms. Heat capacity of lyophilised biomass of Fusarium oxysporum was measured using modulated differential scanning calorimeter. The heat capacity for F. oxysporum grown in cyanidation wastewater was 1.1982, 1.077 and 1.143 J K-1 g-1 on glucose (GA), Beta vulgaris (BA) and cyanide supplemented with Beta vulgaris (BCN), respectively at 298.15 K and 1 atm. The enthalpy of formation of dry biomass are -297.58, -233.07 and -278.60 kJ/C-mol for BA, BCN and GA, respectively. These values were found to be within the range of some biological molecules. The presence of cyanide in the wastewater minimally affected the thermodynamic property of the dried biomass of F. oxysporum.

1 Introduction

There are several reports on microbial treatment of cyanidation wastewater with successful operational efficiency [1-4]. The impact of various factors such as temperature, pH, substrate and bioreactor configuration on the performance of organisms in cyanidation wastewater have been reported [5-7]. In addition, thermodynamic tools have been used to validate the microbial performance and the cyanide degraded [8-10]. However, the uptake of the microbial remediation by the industry have not been inspiring even though Homestake and LaRonde gold mine in Canada, including Gold Fields Limited have demonstrated the robustness and feasibility of the biological process [11-13]. Analysis of process performance should not only be based on microbial growth and toxicant degraded but also on the impact of the toxicant on the physical properties of the organism. This will provide further insight on the capability of the organism to manage their environment under stress.

Thermodynamic properties of a material are an essential tool for predicting the feasibility of any chemical and biological reaction including processes such as the microbial growth process and the biomass conversion of nutrient media to useful products. Among these thermodynamic properties, heat capacity of biological molecules such as starch, glucose, proteins and amino acids reportedly measured based on rudimentary heat capacity quantifications can be used to estimate entropy increments and/or changes at low temperatures (0 to 298.15 K); however, there is high uncertainty associated with this estimate [14]. Recently, some researchers have reported on the use of an adiabatic calorimeter for measuring heat capacity of biological materials at low temperature; based on the application of the third law of thermodynamics, for which incremental entropy and/or absolute entropy can be estimated [15, 16]. Nevertheless, the results were determined to be unreproducible because there was no reference material used and that each researcher had to fabricate their

own calorimeter. This maybe the reason for Pyda's [15] preference for Differential Scanning Calorimeter (DSC) measurements over adiabatic calorimeter measurements. Overall, there is only one report on heat capacity of microbial dried biomass thus far [17] which reported on the use of an adiabatic calorimeter for quantifying the heat capacity of lyophilised cells of *Saccharomyces cerevisiae,* subsequent to the estimation of entropy changes as a function of temperature based on the third law of thermodynamics.

From the second law of thermodynamics, the heat capacity of any material can be estimated/quantified using heat flow curves obtained from DSC generated profiles of the sample being studied. A DSC provides a more reliable, accurate and reproducible results because it is calibrated with a standard reference and/or material such as sapphire, which is used to ascertain and/or detect any error with the equipment, a parametric requirement not available with an adiabatic calorimeter. Nevertheless, it is often difficult to interpret the heat flow data from DSC experiments when multiple processes are involved, resulting in overlapping transitions. Besides, the heat capacity of a material cannot be determined directly from DSC data, it requires multiple experiments including data interpretation to ascertain or determine the heat capacity [18-21].

Furthermore, a modulated DSC (MDSC^{TM}) overcomes these drawbacks and thus provide an insight into the thermal properties of materials being studied. MDSC^{TM} uses a modulated temperature input signal to provide information on the heat capacity, both under isothermal and non-isothermal conditions. Further details on theory, principles, application and instrumentation requirements of the MDSC^{TM} can be found in Vendonck [18] and Knopp [22].

Cells are known to be insoluble and using lyophilised cells, an approximate entropy per unit mass can be obtained if cellular integrity is not annihilated by lyophilisation [23]. Battley [24] in his report hypothesized that the constituent materials of formation do not affect the molecular weight and subsequently thermodynamic properties of lyophilised cell but Duboc et al [25] and Akinpelu et al [26] have proven otherwise with their report on several yeast, bacteria, algae and filamentous fungi. And this agrees with the basic concept that the specific heat is a function of the property of the substance. Therefore, the objective of this study was to determine the impact of different substrates (glucose, *Beta vulgaris* and cyanide) on the heat capacity of lyophilised biomass of*Fusarium oxysporum* in cyanidation wastewater using a modulated DSC (MDSC^{TM}).

2. Materials and methods

2.1 Sample preparation

Carbon sources; glucose (GA), *Beta vulgaris* (BA), and *Beta vulgaris* with cyanide (BCN) were used for the cultivation of*Fusarium oxysporum* in gold mine wastewater as shown in [26]. Briefly, *Fusarium oxysporum* was grown in a 1 litre continuously stirred tank reactor (CSTR) containing metal-laden synthetic gold mine wastewater at 25±2°C. The wastewater contains (per litre): 47 mg $CuSO_45H_2O$, 42 mg $Fe_2(SO_4)_3$ H2O, 278 mg $(NH_4)_2SO_4$, 27mg KH_2PO_4, 3mg $ZnSO_47H_2O$, 0.9 mg $PbBr_2$, and 40 mg Na_2HAsO_4 $7H_2O$. The reactor was inoculated with 10% (v/v) *F. oxysporum* and 0.3 g glucose as refined carbon source. Subsequently, experiments on 0.3 g pulverised *B. vulgaris* followed by 0.3 g pulverised *B. vulgaris* with 100 ppm CN^-/L in form of KCN. Biomass was harvested once the carbon source was used up and/or when the microbial growth reached stationary phase. The harvested biomass was centrifuge at 4°C for 10 min at a speed of 10,000rpm in an Avanti® J-E centrifuge (Beckman Coulter, Inc. USA). Recovered biomass were washed thrice in sterile distilled water, dried in a Duran® vacuum desiccator (DURAN Group GmbH, Germany), and stored at -20 °C for further analyses.

Sample dried biomass was dissolved in sterile distilled water in a 1:1, weight: volume ratio and incubated at 298.15 K for 16 h to ferment any residual carbohydrates. The Durham tube method was used to test for any residual carbohydrates in the suspension [24]. The procedures were repeated until an appropriate quantity of dry biomass was obtained. The elemental analysis of the samples was determined by a Thermo Flash EA 1112 series analyser in a Helium carrier gas (Thermo Fisher Scientific Inc. Waltham, USA) subsequent to estimation of molar mass of dried biomass containing a unit carbon as 23.03, 33.14 and 27.06 g/C-mol for GA, BA and BCN samples, respectively. The detailed elemental analysis of the samples are presented in [26].

2.2 Combustion calorimetry

The heat of combustion of the samples was determined in an e2k Bomb calorimeter (Digital Data Systems Pty Ltd, South Africa) in triplicates as described in [26]. Briefly, a pre-cut firing cotton (Part No. CAL2K-4-FC) was looped over the firing wire (Part No. CAL2K-4-FW) and twisted at the ends. A crucible containing 0.30 g of dried biomass was inserted into the outside electrode's crucible holder, with the firing cotton touching the sample. The electrode assembly was loaded into the vessel body and filled with 3000 kPa oxygen. The vessel was removed from the filling station and allowed to stabilize for 1 min prior to insertion into the calorimeter. The analytical grade Benzoic acid (Part No. CAL2K-BA) was used for calorimeter calibration.

2.3 Modulated differential scanning calorimeter (MDSC)

The MDSC^{TM} uses both the linear heating rate as well as a modulated (sinusoidal) heating rate to determine the total heat flow rate, see Eq. 1. The linear heating rate provides information on the total heat rate while the sinusoidal heating rate provides the heat capacity information from a fraction of the heat flow [27].

$$\frac{\mathrm{dQ}}{\mathrm{dt}} = C_P\beta + f\,(T,\ t) \tag{1}$$

Where $\frac{(dQ}{dt)}$ is the total heat flow due to the linear heating rate (equivalent of standard DSC), C_P is the heat capacity component calculated from the heat flow due to the sinusoidal heating rate, β is the linear heating rate of the sample,$C_P\beta$ is the reversing heat flow while $f(T,\ t)$ is the kinetic component of total heat flow known as the non-reversing heat flow which can be calculated from the difference between the reversing heat flow and total heat signal component.

In this study, a Discovery DSC® (TA Instruments, Inc. New Castle, DE, USA) equipped with a modulated Differential Scanning Calorimeter (MDSC^{TM}) software using a Liquid Nitrogen Cooling Accessory (LNCA) at atmospheric pressure was used for all measurements. Helium gas at a flow rate of 50 mL/min was purged through the MDSC^{TM}. The MDSC^{TM} equilibrated at a temperature of -150 @C and measurements were performed at an underlying heating rate of 3 K/min up to a temperature of 100 @C; amplitude of modulation 1 K and period of 60 s for the sample mass of 2 mg – dry biomass weight. Temperature and heat capacity calibrations were performed with a MDSC^{TM} certified Indium reference material (Part No. 915061.901) and a sapphire for the specific heat capacity determinations (Part No. 9703790.901), respectively at similar operating conditions as used for the samples. The data were analysed using a TRIOS software v4.1.1.33073 (TA Instruments Inc. USA). All procedures were done in triplicate. All dataset are openly available in [28].

3. Results and discussion

3.1 Phase transition

MDSC^{TM} allows for separation and evaluation of thermodynamic and kinetic processes within the regions of glass and melting transitions as shown in equation (1). Endothermic or exothermic enthalpy relaxation may occur within the glass transition range owing to changes in the temperature of the sample. There was no glass transition (T_g) on total heat flow and non-reversible heat flow profiles except on reversible heat flow profiles for all biomass samples tested. There was glass transition (T_g) at a temperature of 239 K and the enthalpy change of 12.586 J/g with an endothermic peak temperature of 292.333 K for BA sample, and a T_g of 211 K, an enthalpy change of 22.096 J/g at an endothermic peak temperature of 287 K for BCN samples on the reversible heat flow profiles which was an indication of a structural transformation of the samples studied, i.e. BA and BCN samples; that is reversible with any temperature changes [29, 30]. The lower T_g for BCN samples is an indication of a rapid breakdown of aromatic constituents in *Beta vulgaris* supplemented biomass owning to the residual free cyanide within the synthetic wastewater used, thereby enhancing microbial growth during the free cyanide biodegradation process. In addition, melting transition (T_m) was observed on the reversing heat flow profiles for all samples studied – see Table 1.

Table 1: Effect of melting temperature on the samples

Samples	T_m (onset) (K)	T_m (peak) (K)	H (J/g)
GA	218.72±1.05	277.113±0.9	17.476±1.01
BA	212.311±1.02	292.333±1.01	12.586±0.8
BCN	127.341±1.04	287.729±1.03	22.096±1.05

Microbial degradation is directly affected by T_m , i.e. the lower the T_m , the higher the biodegradation of a toxicant such as free cyanide [31-33]. *Beta vulgaris* consist of 9.56 % carbohydrates, with betalains, phenolic compounds, including trace elements and minerals accounting for a larger percentage [34, 35]. The presence of betalains and phenolic compounds influence the microbial growth in BA samples since they degrade under different bioreactor operating conditions [36] from that of free cyanide, resulting in a slightly higher molecular weight of the *F. oxysporum* and thus, a higher T_m for BA samples. Similarly, interactions of molecular chains affect the change of enthalpy (H) in melting with the internal energy accounting for the flexibility or otherwise of the samples studied, thus affecting the change of entropy (S) in melting [37]. The highest H in melting for BCN samples was an indication of highest molecular interactions during free cyanide biodegradation.

Tan et al. [30] reported glass transition on reversible heat flow profile of MDSC^{TM}after the onset temperature which overlapped with the peak temperature. It was presumed that this was due to changes in the state of the starch molecules i.e. from being highly confined within the granular packing, to being disentangled as the order in which the molecules are arranged changed as the transition occurred. Glass transition could also be due to structural transitions of cellular materials at temperatures below freezing point of pure water including the influence of the underlying heating rate, modulation period and amplitude [17, 27]. There was no glass transition on*F. oxysporum* grown on glucose i.e. GA, this is similar to the previous report on the heat capacity of starch and glucose [14, 16]. It was evident that the substrate from which the biomass materials were formed, played a major role in the phase transition as can be seen that only cultures grown on *Beta vulgaris* (BA and BCN), had a glass transition.

3.2 Heat capacity

Heat capacity measurements were obtained from 130 to 305 K. The experimental result of the specific heat capacity of Sapphire indicated a general deviation within ±2 percent of standard value as shown in Table 2.

Table 2: Comparison of standard and experimental heat capacity of Sapphire

Temperature (K)	Literature value $\left(JK^{-1}g^{-1}\right)$ [38]	Experimental value $\left(JK^{-1}g^{-1}\right)$	Deviation (%)
130	0.2349	0.2305±0.02	-1.873
140	0.2739	0.2685±0.01	-1.971
150	0.3134	0.3142±0.04	+0.255
160	0.3526	0.3530±0.05	+0.113
170	0.3913	0.3909±0.02	-0.102
180	0.4291	0.4218±0.03	-1.701
190	0.4659	0.4662±0.01	+0.064
200	0.5014	0.4999±0.01	-0.299
220	0.5684	0.5679±0.05	-0.088
230	0.5996	0.6001±0.04	+0.083
250	0.6579	0.6505±0.04	-1.125
270	0.7103	0.7120±0.02	+0.239
273.15	0.7180	0.7167±0.03	-0.181
280	0.7343	0.7353±0.02	+0.136
290	0.7572	0.7561±0.01	-0.145
300	0.7788	0.7775±0.03	-0.167

An indication that the experimental procedure and results are reliable. The experimental specific heat capacity of lyophilised cells of *F. oxysporum* samples in the temperature range of 130 to 305 K are presented in Fig. 1.

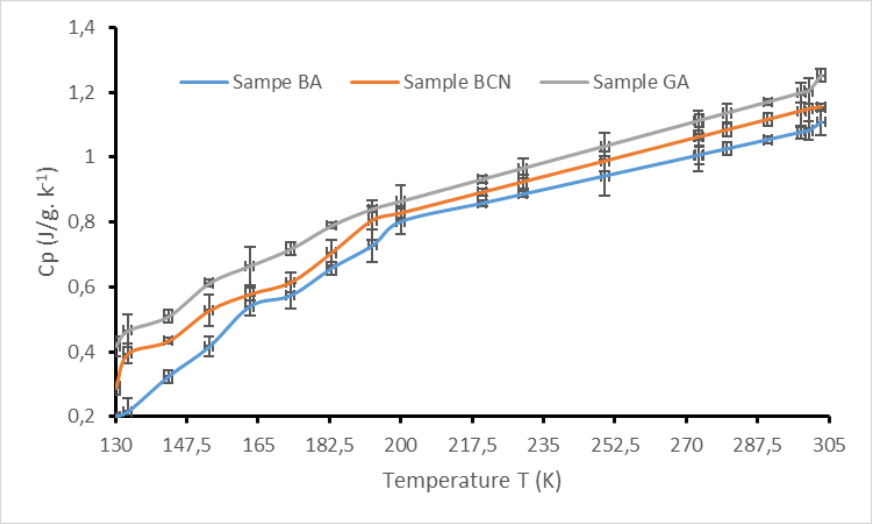

Figure 1 . Heat capacity of samples as a function of temperature

Although there are no general statements on heat capacity changes, the heat capacity of the samples increased steadily with rise in temperature. The heat capacity shows a linear relationship with temperature over the range of (190 to 300) K as shown in equations (2), (3) and (4), respectively.

$$BA: \ C_p\left(\text{J. } K^{-1}g^{-1}\right) = 0.2422 + 0.0028\ T\ \ (K) \tag{2}$$

$$BCN: \ C_p\left(\text{J. } K^{-1}g^{-1}\right) = 0.1889 + 0.0032\ T\ \ (K) \tag{3}$$

$$GA: \ C_p\left(\text{J. } K^{-1}g^{-1}\right) = 0.1845 + 0.0034\ T\ \ (K) \tag{4}$$

The heat capacity of GA samples was shown to be the highest. The low heat capacity observed for BCN samples maybe due to the stress imposed by the free cyanide during microbial proliferation which in turn could affect the biomass structural integrity compared to GA samples. Furthermore, BA samples recorded the lowest heat capacity when compared with all other samples studied. This was expected since *Beta vulgaris* contains approximately 9.56 % carbohydrate that served as an energy and/or carbon source for the *F. oxysporum* used [34, 35]. The higher values of heat capacity in BCN samples when compared to BA samples, could be directly related to the microorganism's ability to utilise cyanide as a carbon source to supplement carbohydrates in *B. vulgaris* agro-industrial waste. Since there is no other reports on heat capacities of microbial dried biomass in literature particularly for fungi, comparing the heat capacity of *Fusarium oxysporum* with *Saccharomyces cerevisiae* showed that from the results obtained, GA samples were comparatively similar to those reported by Battley [17].

Table 3 compares the values of specific heat capacities of starch and/or glucose samples reported by previous authors. At temperature range of (200 to 300) K, our result is closer to the Boerio-Goates report [14] especially GA sample. All the specific heat capacity reported by [17] were higher than our findings while [16] is lower than our reports for BCN and GA samples. Generally, our report can be seen within the reported heat capacity for starch in literature.

Table 3: Comparison of specific heat capacities (J $K^{-1}g^{-1}$) for organic samples

Temp	BA	BCN	GA	Starch	Yeast	Glucose	Starch
(K)	This study	This study	This study	[16]	[17]	[14]	[15]
200	0.8022±0.04	0.8289±0.02	0.8645±0.05	0.7332	0.9040	0.8230	0.7658
250	0.9422±0.06	0.9889±0.03	1.0345±0.04	0.9352	1.1070	1.0162	0.9513
298.15	1.077±0.02	1.1430±0.05	1.1982±0.03	1.1417	1.2990	1.2099	1.1523
300	1.0822±0.03	1.1489±0.06	1.2045±0.04	1.1500	1.3080	1.2171	1.1601

Although, previous study on propagation of *Fusarium oxysporum*showed preference for *Beta vulgaris* with substantial free cyanide biodegradation including diauxic growth [1]. Battley [17] acknowledged that the results are not reproducible, due to the use of an adiabatic calorimeter. However, the results reported herein; i.e. from a MDSC^{TM} are generally deemed reliable thus reproducible. Albeit, if sufficient quantities of *B .vulgaris* and/or further pre-treatment of agro-industrial waste besides pulverising were used, better biodegradation and substrate utilisation performance could have been observed, as this influenced the integrity and the quality of the biomass being generated thus bioreactor performance. As such, it is feasible to suggest that a highly stressful environment culminates in poorly structured cells, which can impede the ability of such cells to detoxify a highly contaminated environment.

3.2 Elemental and combustion analysis

The elemental analysis of the dried biomass samples in percentages of$C$, H , N , and O were determined to give an empirical formula representing the energy constituent of the biomass. Phosphorus and sulphur are not normally included because they do not play any important role in the material balance of cellular reactions and their oxides are part of the ash formed on combustion, thus they are ignored in empirical formulation [17]. The empirical formula of the biomass containing a unit carbon for BA, BCN and GA samples are$CH_{2.377}N_{0.091}O_{1.093}$, $CH_{1.82}N_{0.027}O_{0.804}$, and$CH_{1.167}N_{0.067}O_{0.558}$, with molecular weight of 33.14, 27.06 and 23.03 g/C-mol, respectively [26] which aligns with the previous report for dry biomass[24, 25]. The enthalpy of combustion(H_C^o) of dry biomass in bomb calorimeter is presented in Table 4 based on the reactions (5), (6) and (7) below:

$$BA: CH_{2.377}N_{0.091}O_{1.093}\,(\text{cell}) + 1.048O_{2(g)} \rightarrow \text{CO}_{2(g)} + 1.189H_2O_{(l)} + 0.046N_{2(g)} \quad (5)$$

$$BCN: CH_{1.82}N_{0.027}O_{0.804}\,(\text{cell}) + 1.053O_{2(g)} \rightarrow \text{CO}_{2(g)} + 0.91H_2O_{(l)} + 0.0135N_{2(g)} \quad (6)$$

$$GA: \; CH_{1.167}N_{0.067}O_{0.558}\,(\text{cell}) + 1.0127O_{2(g)} \rightarrow \text{CO}_{2(g)} + 0.5835H_2O_{(l)} + 0.0335N_{2(g)} \quad (7)$$

Table 4: Enthalpy of combustion and formation of dry biomass at 298.15 K and 1 atm.

Microorganisms	Elemental formula	$H_C^o(\frac{\text{KJ}}{C-mol})$	$H_f^o(\frac{\text{KJ}}{C-mol})$	Reference
BA	$CH_{2.377}N_{0.091}O_{1.093}$	-435.78±1.04	-297.58±1.01	This study
BCN	$CH_{1.82}N_{0.027}O_{0.804}$	-420.5±1.76	-233.07±0.98	This study
GA	$CH_{1.167}N_{0.067}O_{0.558}$	-281.69±0.47	-278.60±1.02	This study
A. niger	$CH_{1.5}N_{0.12}O_{0.53}$	-418.7		[25]
Rocan I	$CH_{1.4}N_{0.04}O_{0.5}$	-473.3		[25]
B. flavum	$CH_{1.8}N_{0.19}O_{0.33}$	-491.7		[25]
S. cerevisiae	$CH_{1.613}N_{0.158}O_{0.557}$	-509.37	-133.13	[24]

The enthalpy of combustion of the samples agree with the previous reports except for the sample GA. The reason for this deviation is not clear. The enthalpy of formation (H_f^o) for each sample was calculated using standard heat of formation$H_f^o\left(\text{CO}_{2(g)}\right) = -393.51\ kJ/mol$ and$H_f^o\left(H_2O_{(l)}\right) = -285.83\ kJ/mol$[24], according to the reactions (5), (6) and (7).

The accuracy of these values (H_f^o) is a function of the validity of the molecular formula of the carbohy-

drate used to represent the *B. vulgaris* agro-waste which has a direct influence on the accuracy of the heat determination. Environmental factors such as temperature, pH, substrate concentration and presence of toxins have been used extensively to elucidate the feasibility of microbial degradation. Estimation of physical property such as heat capacity and heat of formation will further ascertain the veracity of microorganism in environmental engineering application.

4. Conclusion

The results presented herein showed that the substrate used for microbial growth can affect the determination of the heat capacity as well as enthalpy of biological samples. The determination of such heat capacity of a material as a function of the structure of the material can assist in substrate selection for cyanidation wastewater treatment. The impairment caused by free cyanide also reflected on the heat capacity and enthalpy of dry biomass assessed. The toxicity by free cyanide reduces the biomass molecular degree of freedom hence, the biomass could not store sufficient thermal energy as most energy resources are dedicated for cellular maintenance. The enthalpy of combustion of dried biomass of *F. oxysporum* is within the range available in literatures. This suggests that the method of biomass preparation and its constituents does not significantly affect the final enthalpy of biomass formation. Since biomass are not completely crystalline substance, the enthalpy derived from the calorimetric measurement can be used to further elucidate the capabilities associated with the novel biocatalyst selection for the bioremediation of cyanidation wastewater.

Acknowledgements

The authors acknowledge Ross Burnham of Advanced Laboratory Solutions for his assistance on DSC data interpretation and the funding from the Cape Peninsula University of Technology (CPUT), University Research Fund (URF RK 16).

Conflict of interest

The authors declare no financial or commercial conflict of interest

References

[1] E.A. Akinpelu, S.K.O. Ntwampe, L. Mekuto, E.F. Itoba Tombo, Optimizing the bioremediation of free cyanide containing wastewater by *Fusarium oxysporum* grown on beetroot waste using response surface methodology, in: S.I. Ao, C. Douglas, W.S. Grundfest (Eds.) Lecture Notes in Engineering and Computer Science: Proceedings of the World Congress on Engineering and Computer Science, Newswood Limited, San Francisco, USA, 2016, pp. 664-670.

[2] L. Mekuto, S.K.O. Ntwampe, C.E. Utomi, M. Mobo, J.B. Mudumbi, M.M. Ngongang, E.A. Akinpelu, Performance of a continuously stirred tank bioreactor system connected in series for the biodegradation of thiocyanate and free cyanide, Journal of Environmental Chemical Engineering, 5 (2017) 1936-1945.

[3] V.K. Virender Kumar, T.C. Bhalla, In vitro cyanide degradation by Serretia marcescens RL2b, Int J Environ Sci, 3 (2013).

[4] K.K. Ibrahim, M.A. Syed, M.Y. Shukor, S.A. Ahmad, Biological Remediation of Cyanide: A Review, BIOTROPIA-The Southeast Asian Journal of Tropical Biology, 22 (2016) 151-163.

[5] M.G. Campos, P. Pereira, J.C. Roseiro, Packed-bed reactor for the integrated biodegradation of cyanide and formamide by immobilised *Fusarium oxysporum* CCMI 876 and*Methylobacterium sp.* RXM CCMI 908, Enzyme and Microbial Technology, 38 (2006) 848-854.

[6] V.M. Luque-Almagro, C. Moreno-Vivián, M.D. Roldán, Biodegradation of cyanide wastes from mining and jewellery industries, Current Opinion in Biotechnology, 38 (2016) 9-13.

[7] L. Mekuto, S. Ntwampe, V. Jackson, Biodegradation of free cyanide and subsequent utilisation of biodegradation by-products by Bacillus consortia: optimisation using response surface methodology, Environ Sci Pollut Res, 22 (2015) 10434-10443.

[8] E.A. Akinpelu, S.K. Ntwampe, N. Mpongwana, F. Nchu, T.V. Ojumu, Biodegradation Kinetics of Free Cyanide in *Fusarium oxysporum-Beta vulgaris* Waste-metal (As, Cu, Fe, Pb, Zn) Cultures under Alkaline Conditions, BioResources, 11 (2016) 2470-2482.

[9] A. Behnamfard, M.M. Salarirad, Equilibrium and kinetic studies on free cyanide adsorption from aqueous solution by activated carbon, Journal of Hazardous Materials, 170 (2009) 127-133.

[10] N. Singh, C. Balomajumder, Equilibrium isotherm and kinetic studies for the simultaneous removal of phenol and cyanide by use of *S. odorifera* (MTCC 5700) immobilized on coconut shell activated carbon, Applied Water Science, (2016) 1-15.

[11] R.J. Huddy, A.W. van Zyl, R.P. van Hille, S.T.L. Harrison, Characterisation of the complex microbial community associated with the ASTER thiocyanate biodegradation system, Minerals Engineering, 76 (2015) 65-71.

[12] M.B. Stott, P.D. Franzmann, L.R. Zappia, H.R. Watling, L.P. Quan, B.J. Clark, M.R. Houchin, P.C. Miller, T.L. Williams, Thiocyanate removal from saline CIP process water by a rotating biological contactor, with reuse of the water for bioleaching, Hydrometallurgy, 62 (2001) 93-105.

[13] C. Du Plessis, P. Barnard, R. Muhlbauer, K. Naldrett, Empirical model for the autotrophic biodegradation of thiocyanate in an activated sludge reactor, Letters in Applied Microbiology, 32 (2001) 103-107.

[14] J. Boerio-Goates, Heat-capacity measurements and thermodynamic functions of crystalline α-D-glucose at temperatures from 10 K to 340 K, The Journal of Chemical Thermodynamics, 23 (1991) 403-409.

[15] M. Pyda, Conformational contribution to the heat capacity of the starch and water system, Journal of Polymer Science Part B: Polymer Physics, 39 (2001) 3038-3054.

[16] G.J. Kabo, O.V. Voitkevich, A.V. Blokhin, S.V. Kohut, E.N. Stepurko, Y.U. Paulechka, Thermodynamic properties of starch and glucose, The Journal of Chemical Thermodynamics, 59 (2013) 87-93.

[17] E.H. Battley, R.L. Putnam, J. Boerio-Goates, Heat capacity measurements from 10 to 300 K and derived thermodynamic functions of lyophilized cells of Saccharomyces cerevisiae including the absolute entropy and the entropy of formation at 298.15 K, Thermochimica Acta, 298 (1997) 37-46.

[18] E. Verdonck, K. Schaap, L.C. Thomas, A discussion of the principles and applications of Modulated Temperature DSC (MTDSC), Int. J. Pharm., 192 (1999) 3-20.

[19] W.A. Brantley, M. Iijima, T.H. Grentzer, Temperature-modulated DSC provides new insight about nickel-titanium wire transformations, American Journal of Orthodontics and Dentofacial Orthopedics, 124 (2003) 387-394.

[20] F. Xie, W.-C. Liu, P. Liu, J. Wang, P.J. Halley, L. Yu, Starch thermal transitions comparatively studied by DSC and MTDSC, Starch - Stärke, 62 (2010) 350-357.

[21] A. Magoń, M. Pyda, Apparent heat capacity measurements and thermodynamic functions of d(-)-fructose by standard and temperature-modulated calorimetry, The Journal of Chemical Thermodynamics, 56 (2013) 67-82.

[22] M.M. Knopp, K. Löbmann, D.P. Elder, T. Rades, R. Holm, Recent advances and potential applications of modulated differential scanning calorimetry (mDSC) in drug development, Eur. J. Pharm. Sci., 87 (2016) 164-173.

[23] E.H. Battley, Energetics of microbial growth, Wiley Inter-science, New York, 1987.

[24] E.H. Battley, The thermodynamics of microbial growth, in: R.B. Kemp (Ed.) Handbook of thermal analysis and calorimetry, Elsevier, Amsterdam, 1999, pp. 219-266.

[25] P. Duboc, I. Marison, U. Von Stockar, Quantitative calorimetry and biochemical engineering, in: R.B. Kemp (Ed.) Handbook of thermal analysis and calorimetry, Elsevier, Amsterdam, 1999, pp. 267-365.

[26] E.A. Akinpelu, S.K.O. Ntwampe, B.-H. Chen, Biological stoichiometry and bioenergetics of Fusarium oxysporum EKT01/02 proliferation using different substrates in cyanidation wastewater, The Canadian Journal of Chemical Engineering, 96 (2018) 537-544.

[27] W. Stark, M. Jaunich, J. McHugh, Cure state detection for pre-cured carbon-fibre epoxy prepreg (CFC) using Temperature-Modulated Differential Scanning Calorimetry (TMDSC), Polym. Test., 32 (2013) 1261-1272.

[28] E. Akinpelu, S. Ntwampe, L. Mekuto, T. Ojumu, Thermodynamic Data of *Fusarium oxysporum* Grown on Different Substrates in Gold Mine Wastewater, Data, 2 (2017) 24.

[29] V.-F. Lai, C.-Y. Lii, Effects of modulated differential scanning calorimetry (MDSC) variables on thermodynamic and kinetic characteristics during gelatinization of waxy rice starch, Cereal chemistry, 76 (1999) 519-525.

[30] I. Tan, C.C. Wee, P.A. Sopade, P.J. Halley, Investigation of the starch gelatinisation phenomena in water–glycerol systems: application of modulated temperature differential scanning calorimetry, Carbohydrate Polymers, 58 (2004) 191-204.

[31] K. Herzog, R.J. Müller, W.D. Deckwer, Mechanism and kinetics of the enzymatic hydrolysis of polyester nanoparticles by lipases, Polym. Degradation Stab., 91 (2006) 2486-2498.

[32] R.-J. Mueller, Biological degradation of synthetic polyesters—Enzymes as potential catalysts for polyester recycling, Process Biochem., 41 (2006) 2124-2128.

[33] K.-i. Kasuya, N. Ishii, Y. Inoue, K. Yazawa, T. Tagaya, T. Yotsumoto, J.-i. Kazahaya, D. Nagai, Characterization of a mesophilic aliphatic–aromatic copolyester-degrading fungus, Polym. Degradation Stab., 94 (2009) 1190-1196.

[34] J. Wruss, G. Waldenberger, S. Huemer, P. Uygun, P. Lanzerstorfer, U. Müller, O. Höglinger, J. Weghuber, Compositional characteristics of commercial beetroot products and beetroot juice prepared from seven beetroot varieties grown in Upper Austria, Journal of Food Composition and Analysis, 42 (2015) 46-55.

[35] USDA, USDA National Nutrient Database for Standard Reference Release 28, USDA, USA, 2016.

[36] K.M. Herbach, F.C. Stintzing, R. Carle, Betalain Stability and Degradation—Structural and Chromatic Aspects, J. Food Sci., 71 (2006) R41-R50.

[37] Y. Tokiwa, B. Calabia, C. Ugwu, S. Aiba, Biodegradability of Plastics, International Journal of Molecular Sciences, 10 (2009) 3722.

[38] D. Ditmars, S. Ishihara, S. Chang, G. Bernstein, E. West, Enthalpy and heat-capacity standard reference material: synthetic sapphire (α-Al_2O_3) from 10 to 2250 K, J. Res. Natl. Bur. Stand, 87 (1982) 159-163.